Improved diagnosis of the number of stenosed coronary artery vessels by segmentation with scatter and photo-peak window data for attenuation correction in myocardial perfusion SPECT

Yohei Yamauchi, MD,[a] Yumiko Kanzaki, MD,[a] Masuo Hayashi, RT,[b] Mami Arai, RT,[b] Hideaki Morita, MD,[a] Tsuyoshi Komori, MD,[b] Masaaki Hoshiga, MD,[a] and Nobukazu Ishizaka, MD[a]

[a] Department of Cardiology, Osaka Medical College, Takatsuki, Japan
[b] Department of Radiology, Osaka Medical College, Takatsuki, Japan

Received May 2, 2017; accepted Aug 22, 2017
doi:10.1007/s12350-017-1058-x

Background. **Attenuation correction using segmentation of scatter and photo-peak window data (SSPAC) enables an evaluation of the attenuation map in a patient-specific manner without additional radiation exposure. We compared the accuracy of SSPAC and non-corrected myocardial perfusion scintigraphy methods for diagnosing the number of stenosed coronary artery vessels.**

Methods and Results. **We retrospectively reviewed the data from 183 consecutive patients who underwent ^{99m}Tc-tetrofosmin stress/rest SPECT examination and a coronary angiography within 3 months. The MPS images were reconstructed with and without SSPAC attenuation correction. We examined the accuracy of the quantitative interpretation using summed differential score in the detection of coronary artery disease (CAD). The attenuation maps were successfully determined in 179 of 183 patients (98%). In terms of the vessel-based diagnostic ability, sensitivity, specificity, positive predictive and negative predictive values of the SSPAC and non-correction methods for diagnosing CAD in individual coronary territories were 77%*, 89%, 74%*, and 90%* vs 51%, 87%, 62%, and 82%, respectively (**P* < .05). In 35 patients with multi-vessel CAD, those values were 78%*, 81%, 93%, and 55%* vs 49%, 81%, 89%, and 34%, respectively (**P* < .05; AUC: 0.82 vs 0.62, *P* < .05).**

Conclusion. **SSPAC-corrected SPECT myocardial perfusion images exhibit improved accuracy in the detection of the number of stenosed coronary artery vessels, even in patients with multi-vessel CAD. (J Nucl Cardiol 2019;26:574–81.)**

Key Words: SSPAC • SPECT • Attenuation correction • Invasive coronary angiography • Coronary artery disease

See related editorial, pp. 582–584

Electronic supplementary material The online version of this article (doi:10.1007/s12350-017-1058-x) contains supplementary material, which is available to authorized users.

The authors of this article have provided a PowerPoint file, available for download at SpringerLink, which summarizes the contents of the paper and is free for re-use at meetings and presentations. Search for the article DOI on SpringerLink.com.

Reprint requests: Yumiko Kanzaki, MD, Department of Cardiology, Osaka Medical College, 2-7, Daigaku-machi, Takatsuki 569-8686, Japan; *in3089@osaka-med.ac.jp*

1071-3581/$34.00

Abbreviations

SSPAC	Segmentation with scatter and photo-peak window attenuation correction
MPS	Myocardial perfusion SPECT
MPI	Myocardial perfusion imaging
SPECT	Single-photo emission computed tomography
QGS	Quantitative gated SPECT
EF	Ejection fraction
EDV	End-diastolic volume
ESV	End-systolic volume
SDS	Summed difference score
AUCs	Area under the curves

INTRODUCTION

Although stress myocardial perfusion scintigraphy (MPS) has a high sensitivity for detecting coronary artery disease (CAD) in patients with multi-vessel CAD,[1–8] it may be less potent in identifying the exact location of the diseased coronary arteries.[9–13] Several attenuation correction methods have been reported that show improved accuracy for identifying the number of narrowing coronary vessels among patients with multi-vessel disease.[14–18] Segmentation with scatter and photo-peak window data for attenuation correction (SSPAC) for single-photon emission computed tomography (SPECT) is a recently developed correction method that utilizes a patient-specific non-uniform attenuation coefficient map.[19,20] We have previously shown that this method provides improved diagnostic accuracy for CAD without additional radiation exposure.[21] In the present study, we investigated whether it is clinically feasible to estimate the number of diseased coronary artery vessels using the SSPAC method.

METHODS

Study Patients

We examined 183 consecutive patients (121 men, 62 women; mean age, 72 ± 8 years) who had no prior myocardial infarction, decompensated congestive heart failure, idiopathic cardiomyopathy, atrial fibrillation, history of cardiac surgery, advanced atrioventricular block, severe chronic obstructive pulmonary disease, or bronchospasm, and who underwent ^{99m}Tc-tetrofosmin stress (physical or adenosine) and rest gated myocardial SPECT together with coronary angiography that was performed within 3 months of the SPECT study between 2012 and 2017. This study was approved by the Ethical Committee of the Osaka Medical College.

Image Acquisition

A 1-day stress and rest SPECT myocardial perfusion imaging (MPI) was performed in all patients. Eighty-nine patients (49%) performed an exercise-stress, and the remaining 94 patients (51%) were pharmacologically stressed (140 µg/kg·min of adenosine for 6 minutes). Twelve-lead electrocardiograms and blood pressure measurements were obtained at baseline and then every minute during exercise. Myocardial SPECT was performed approximately 30–45 minutes after administering a tracer injection of 296 MBq ^{99m}Tc-tetrofosmin using a triple-detector SPECT system (GCA-9300R; Toshiba Medical Systems, Tochigi, Japan) with low-energy high-resolution collimator. Four hours later, resting SPECT was performed approximately 1 hour after an injection of 600 MBq ^{99m}Tc-tetrofosmin. The gated SPECT data were acquired by the following parameters: 360° step-and-shoot rotation, 60 steps, 40 or 60 seconds per step, 128 × 128 matrix (1 pixel = 3.2 mm), 16 frames per cardiac cycle, and a beat acceptance window at 20% of the average RR interval calculated just before the beginning of data collection. The ungated projection data were obtained by summing the gated projection data.

Data Processing and Analysis

The SSPAC method was performed as described previously.[21] The processes of SSPAC and non-correction images are shown in Figure 1. The SSPAC method required the acquisition of scatter window data (7% of the lower side of the emission window) in addition to photo-peak window data (140 keV ± 10%). A patient-specific attenuation correction map was obtained semi-automatically in a few minutes through SSPAC implemented in a GMS-7700b or Vitrea workstation (Toshiba Medical Systems, Tochigi, Japan). The non-correction images were reconstructed by performing filtered back projection from the projection data. The reconstructed short-axis images obtained by the SSPAC and non-correction methods were analyzed using a quantitative perfusion SPECT with gated SPECT software (QPS/QGS, Cedars-Sinai Medical Center, Los Angeles, CA, USA). Perfusion polar maps of 17 segments were generated using QPS software. SSPAC and non-correction databases were calculated using the QPS software. Ejection fraction, end-diastolic volume, and end-systolic volume were obtained using QGS analysis.[22]

Evaluation of Perfusion

The SPECT images from the post-stress and resting studies were displayed on the PC monitor to evaluate myocardial perfusion, and two experienced observers who were blinded to the clinical data examined the images separately. Subsequently, the differences between the readers were resolved using consensus obtained by simultaneously viewing the SPECT images. We evaluated the diagnostic accuracy for the patient-based data and the vessel-based analysis.

A 17-segment model was used to semi-quantitatively evaluate the perfusion defects. Individual segments were

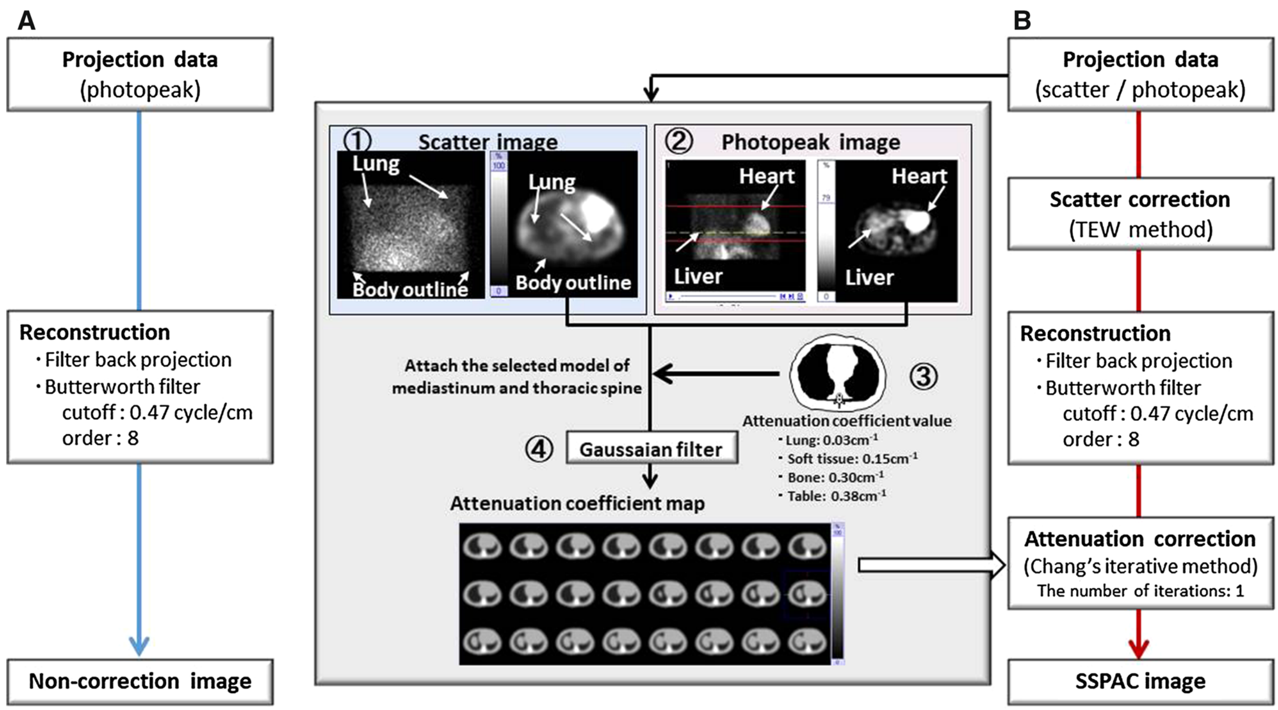

Figure 1. The processes for constructing segmentation with scatter and photo-peak window data for non-correction images and attenuation correction (SSPAC) images. **A** The non-correction images were reconstructed by performing filtered back projection from the projection data. **B** For SSPAC images, a triple-energy window (TEW) scatter correction was performed on the projection data. Those data were reconstructed by performing filtered back. The attenuation correction images were reconstructed by Chang's iterative method using the attenuation coefficient map. ① The body and lung contours were determined from reconstructed scatter window data. ② The myocardium and the liver were determined from reconstructed photo-peak window data. ③ The body outlines, lung contours, myocardium, and liver were attached to models of the average mediastinum and thoracic spine, which were obtained by computed tomography. The attenuation coefficient value according to the influence of absorption was assigned to each organ. ④ A Gaussian filter was applied to the attenuation coefficient map to match to for the system resolution.

scored as follows: 0, normal; 1, mildly reduced; 2, moderately reduced; 3, severely reduced; and 4, absent. The severity of reversible defects in myocardial perfusion was defined based on the summed difference scores (SDSs) derived from summed stress scores and summed rest scores for all the segments. The anterior, apical, and septal walls (1, 2, 7, 8, 13, 14, and 17 segments) were assigned to the left anterior descending artery (LAD), the lateral wall (5, 6, 11, 12, and 16 segments) was assigned to the left circumflex artery (LCx), and the left main trunk (LMT) disease, including both LAD and LCx territories, was assigned to LMT. The inferior and basal septal segments (3, 4, 9, 10, and 15 segments) were assigned to the right coronary artery (RCA).[23] Abnormal MPS results were defined by a score of ≥2 of SDSs based on each coronary territory.

Coronary Angiography

Coronary angiography was performed using standard methods. Coronary stenosis was evaluated using multiple projections by experienced investigators who were unaware of the clinical data including SPECT data. Quantitative coronary angiography (QCA) was performed using QCA-CMS software (MEDIS medical imaging systems, Leiden, The Netherlands). A stenosis was considered significant when >50% lumen narrowing was present.[24,25]

Statistical Analysis

The data are presented as mean ± standard deviation (SD). Paired *t*-tests were used to compare the differences in the paired continuous data, and the χ^2 or Fisher's exact tests were used to compare the differences for the paired discrete data, as appropriate. Sensitivity, specificity, positive predictive value (PPV), and negative predictive value (NPV) in indices were calculated as predictors of significant CAD. The receiver operating characteristic (ROC) curves were generated by calculating the sensitivity and specificity for CAD. JMP 11.0 (SAS Institute, Cary, NC, USA) was used to perform all statistical analyses. A P value <.05 was considered to be significant.

RESULTS

Clinical Characteristics

Using SSPAC method, attenuation coefficient maps could be created for 179 (98%) of the 183 study patients. The characteristics of these 179 patients are described in Table 1. Coronary angiography showed no significant stenosis in the coronary artery of 69 patients, showed single-vessel disease in 75 patients, and multi-vessel disease in 35 patients. Among the patients with multi-vessel disease, eight patients (23%) showed transient ischemic dilatation of >1.12, which was defined as an abnormal ratio.[26,27]

Diagnostic Accuracy of the SSPAC Method

The patient-based diagnostic ability of SSPAC and non-correction images for the detection of CAD is described in Table 2 (AUC 0.81 vs 0.75; $P = .059$), and vessel-based diagnostic ability is shown in Table 3 (AUC 0.83 vs 0.72; $P < .05$).

Non-correction and SSPAC Image for Multi-vessel Disease

Among 35 patients with multi-vessel disease, the accuracy for diagnosing CAD in individual coronary territories is shown in Table 4. Even in patients with multi-vessel disease, the SSPAC method showed significantly higher sensitivity and NPV than the non-correction method. The respective proportion of number of stenosed coronary artery vessels as described at CAG, non-correction, and SSPAC method images were shown in Figure 2. Representative case of the SSPAC and non-correction images for the patient with multi-vessel disease is shown in Figure 3.

Table 2. Patient-based diagnostic ability of SSPAC and non-correction images in the detection of coronary artery disease

	NC (%)	SSPAC (%)
Sensitivity	75	85
Specificity	68	64
Accuracy	73	77
PPV	79	79
NPV	64	72

NC, non-correction method; *PPV*, positive predictive value,;*NPV*, negative predictive value
* $P < .05$

Table 1. Patient characteristics

Parameters	No CAD (n = 69)	SVD (n = 75)	MVD (n = 35)	P
Mean age (years)	72 ± 8	72 ± 8	74 ± 6	NS
Male (n)	40 (58%)	55 (73%)	23 (66%)	NS
BMI (kg/m^2)	23 ± 4	24 ± 3	25 ± 3	NS
Stress protocol (exercise) (n)	30 (43%)	39 (52%)	19 (54%)	NS
Hypertension (n)	55 (80%)	68 (91%)	32 (91%)	NS
Dyslipidemia (n)	37 (54%)	48 (64%)	26 (74%)	NS
Diabetes mellitus (n)	13 (19%)	35 (47%)	17 (49%)	NS
History of smoking (n)	30 (43%)	48 (64%)	16 (46%)	NS
Family history of CAD (n)	8 (12%)	11 (15%)	3 (9%)	NS
LV function at stress				
End-diastolic volume (mL)	63 ± 23	69 ± 21	67 ± 17	NS
End-systolic volume (mL)	21 ± 12	24 ± 12	21 ± 9	NS
Ejection fraction (%)	69 ± 10	66 ± 9	69 ± 9	NS
LV function at rest				
End-diastolic volume (mL)	63 ± 23	68 ± 20	64 ± 17	NS
End-systolic volume (mL)	19 ± 12	22 ± 11	17 ± 8	NS
Ejection fraction (%)	72 ± 10	69 ± 9	74 ± 8	$p < .05$
Transient ischemic dilatation	1.02 ± 0.11	1.02 ± 0.08	1.05 ± 0.09	NS

CAD, coronary artery disease; *SVD*, single-vessel disease; *MVD*, multi-vessel disease; *BMI*, body mass index

Table 3. Vessel-based diagnostic ability of SSPAC and non-correction images in the detection of coronary artery disease in total 537 vessels from 179 patients

			LAD territory		LCx territory		RCA territory	
	NC (%)	SSPAC (%)	NC (%)	SSPAC (%)	NC (%)	SSPAC (%)	NC (%)	SSPAC (%)
Sensitivity	51	77*	47	79*	60	77	47	72*
Specificity	87	89	88	83	93	95	83	88
Accuracy	77	85*	73	82*	83	90	75	85*
PPV	62	74*	69	73	78	87	40	60
NPV	82	90*	74	87*	85	91	86	93

PPV, positive predictive value; *NPV*, negative predictive value; *LAD*, left anterior descending coronary artery territory; *LCx*, left circumflex coronary artery territory; *RCA*, right coronary artery territory; *NC*, non-correction method
* $P < .05$

Table 4. Diagnostic ability of non-correction and SSPAC images in the detection of coronary artery disease based on the territory of vessels in 38 patients with multi-vessel disease

			LAD territory		LCx territory		RCA territory	
	NC (%)	SSPAC (%)	NC (%)	SSPAC (%)	NC (%)	SSPAC (%)	NC (%)	SSPAC (%)
Sensitivity	49	78*	54	89*	46	71	48	74
Specificity	81	81	86	86	57	71	92	83
Accuracy	57	79*	60	89*	49	71*	63	77
PPV	89	93	94	96	81	91	92	89
NPV	34	55*	32	67	21	38	48	63

NC, non-correction method; *PPV*, positive predictive value; *NPV*, negative predictive value; *LAD*, left anterior descending coronary artery territory; *LCx*, left circumflex coronary artery territory; *RCA*, right coronary artery territory
* $P < .05$

DISCUSSION

This study demonstrated that MPS using the SSPAC method has similar specificity but higher sensitivity than the non-correction method in detecting significant coronary artery stenosis lesions, even in patients with multi-vessel disease.

The SSPAC method uses information which merges an atlas-based estimate of the bone structures, a segmented body and lung outline from a scatter window image, and myocardial and liver structure from photopeak image, and soft tissues. The SSPAC method has the advantages of removing the risk of additional radiation exposure and minimizing the deleterious effect of respiratory motion while adding only a few minutes of analysis to construct the map. It has been reported that myocardial perfusion counts become more consistent with the use of SSPAC in normal subjects,[20] and we also reported that the SSPAC method provides better diagnostic accuracy for the detection of CAD, including myocardial infarction using the summed stress score.[20] In the present study, we selected patients who had no prior myocardial infarction; we diagnosed limited ischemic lesions using SDS scores. The SSPAC method also improved the precise per-vessel diagnosis in patients with CAD, and even in those with multi-vessel disease. Such improvement was reflected more clearly in the increased sensitivity in the LAD and RCA territory. We think that the following reasons may explain this: the myocardial perfusion became homogeneous in rest image, and scatter contribution to the apparent uptake in the myocardium was significantly different at rest and stress in their patients; this produces the change in SDS in the SSPAC method. The attenuation in the inferior region was corrected by SSPAC method and the counts in the other regions were corrected relatively. We also propose its combined with the ability to perform scatter correction to improve the contrast in the MPS image.

The sensitivity of stress MPS for detection of the presence of multi-vessel disease is limited.[1,5–8] The possible reasons for this include balanced perfusion abnormality, where the absence of a normal reference segment limits sensitivity; early plateau of tracer uptake,

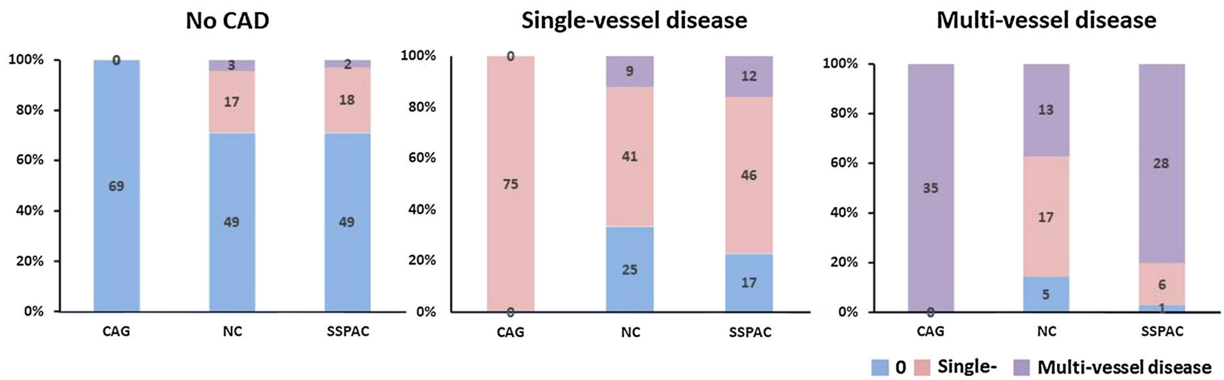

Figure 2. Respective proportion of the number of stenosed coronary artery vessels as described at coronary angiography (CAG), myocardial perfusion image; non-correction (NC) and SSPAC images.

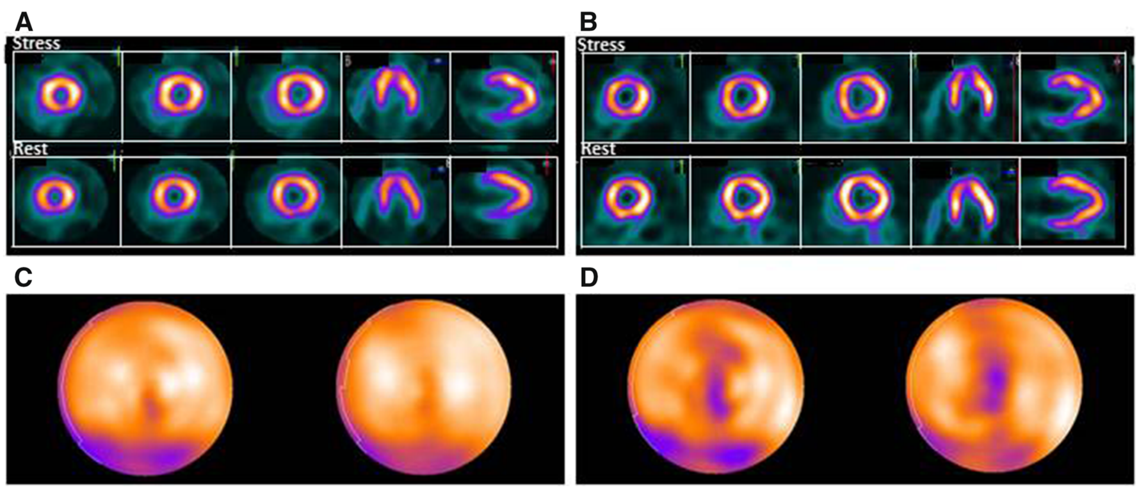

Figure 3. A 68-year-old man with significant stenosis in LAD and RCA. The non-correction myocardial perfusion images (**A**, **C**) reveal reversible defect in only the inferior wall, and images after attenuation correction using the SSPAC method reveal reversible defects in the anterior and inferior walls (**B**, **D**); however, apical thinning is more pronounced.

which limits detection of borderline stenosis; and early stoppage of exercise as a result of signs or symptoms due to the severest lesion.[13] Extensive clinical investigations have been performed for attenuation correction and it is now one of the recommended techniques for improving the image quality of MPS and diagnostic accuracy for detecting CAD.[28–31] Use of attenuation correction for detecting multi-vessel disease is still controversial. Ficaro et al. have reported increased diagnostic accuracy of attenuation-corrected SPECT for diagnosis of multi-vessel disease by simultaneous transmission/emission tomography or computed tomography.[18] In contrast, Hendel et al. showed that among 96 patients with angiographically proven CAD and 88 subjects with low likelihood of CAD, attenuation correction resulted in a significantly higher normalcy rate (86% vs 96%, respectively). However, the sensitivity did not improve with attenuation correction, and for patients with RCA or multi-vessel disease, it was slightly worse in a multi-center trial.[32]

Patients with multi-vessel disease have poor prognosis without revascularization.[33] Underestimation of the extent of ischemia on SPECT MPI is regarded as one of its most important limitations. We thought that it is important to detect multi-vessel disease by MPS. Furthermore, the SSPAC method is suitable for routine attenuation correction at our institute. It is easy to perform and usually requires several minutes or less to construct the patient-specific attenuation map without additional radiation exposure.

Study Limitations

This study has some limitations. First, we were unable to construct attenuation coefficient maps using the SSPAC method for some patients in this study. The primary reason was that it was not possible to detect the outline of the body or lung from scatter image. We thought that patients with the following condition may not be suitable for the SSPAC method: very large patients, cases for which arms must be positioned at the side of the body, lung lobectomy, excessive ^{99m}Tc-tetrofosmine lung uptake, patients with large gastric bubble. Second, our study involved a relatively small number of patients. We need to assess this method over a larger population, especially in patients with multi-vessel diseases, and evaluate its effectiveness according to differences in sex, body mass index, and other parameters. Third, we reconstructed SPECT images using the filtered back projection and Chang's iterative method. We need to assess the accuracy of this method in comparison with the ordered subset expectation maximization method. Fourth, visual assessment is subjective and experience dependent. Fifth, in this study, we used both attenuation and scatter correction to construct SSPAC image. Both these methods may occasionally lead to miscorrection. Further, we did not assess the SSPAC method and scatter correction separately to know the mechanism of improved diagnosis accuracy in stenosed vessels. Finally, the diagnostic criteria for coronary stenosis include stenosis of the coronary arteries according to angiographic findings, not physiological changes, such as the functional flow reserve.[34–37]

CONCLUSIONS

The SSPAC method of stress-induced SPECT may provide improved sensitivity in the presence of stenosed coronary artery vessels, even in patients with multi-vessel CAD.

NEW KNOWLEDGE GAINED

The SSPAC method may be useful for diagnosing in the presence of stenosed coronary artery vessels.

Acknowledgement

We gratefully acknowledge the generous assistance and valuable information of Mr. Kenji Kuse and Mr. Masahiro Kubota, the technical assistance of the staff (Mr. Akira Asazu, and Mr. Hideyuki Sodeoka) in our nuclear medicine department, and the secretary assistance of Ms. Yuko Takenaka and Ms. Megumi Hashimoto.

Disclosure

None.

References

1. Lima RS, Watson DD, Goode AR, Siadaty MS, Ragosta M, Beller GA, et al. Incremental value of combined perfusion and function over perfusion alone by gated SPECT myocardial perfusion imaging for detection of severe three-vessel coronary artery disease. J Am Coll Cardiol 2003;42:64-70.
2. Yamagishi H, Shirai N, Yoshiyama M, Teragaki M, Akioka K, Takeuchi K, et al. Incremental value of left ventricular ejection fraction for detection of multivessel coronary artery disease in exercise (201)Tl gated myocardial perfusion imaging. J Nucl Med 2002;43:131-9.
3. Berman DS, Kang X, Slomka PJ, Gerlach J, de Yang L, Hayes SW, et al. Underestimation of extent of ischemia by gated SPECT myocardial perfusion imaging in patients with left main coronary artery disease. J Nucl Cardiol 2007;14:521-8.
4. Shirai N, Yamagishi H, Yoshiyama M, Teragaki M, Akioka K, Takeuchi K, et al. Incremental value of assessment of regional wall motion for detection of multivessel coronary artery disease in exercise (201)Tl gated myocardial perfusion imaging. J Nucl Med 2002;43:443-50.
5. Travin MI, Katz MS, Moulton AW, Miele NJ, Sharaf BL, Johnson LL. Accuracy of dipyridamole SPECT imaging in identifying individual coronary stenoses and multivessel disease in women versus men. J Nucl Cardiol 2000;7:213-20.
6. Galassi AR, Grasso C, Azzarelli S, Ussia G, Moshiri S, Tamburino C. Usefulness of exercise myocardial scintigraphy in multivessel coronary disease after incomplete revascularization with coronary stenting. Am J Cardiol 2006;97:207-15.
7. Mahajan N, Polavaram L, Vankayala H, Ference B, Wang Y, Ager J, et al. Diagnostic accuracy of myocardial perfusion imaging and stress echocardiography for the diagnosis of left main and triple vessel coronary artery disease: A comparative meta-analysis. Heart 2010;96:956-66.
8. Chung SY, Lee KY, Chun EJ, Lee WW, Park EK, Chang HJ, et al. Comparison of stress perfusion MRI and SPECT for detection of myocardial ischemia in patients with angiographically proven three-vessel coronary artery disease. AJR 2010;195:356-62.
9. Rehn T, Griffith LS, Achuff SC, Bailey IK, Bulkley BH, Burow R, et al. Exercise thallium-201 myocardial imaging in left main coronary artery disease: Sensitive but not specific. Am J Cardiol 1981;48:217-23.
10. Christian TF, Miller TD, Bailey KR, Gibbons RJ. Noninvasive identification of severe coronary artery disease using exercise tomographic thallium-201 imaging. Am J Cardiol 1992;70:14-20.
11. Nygaard TW, Gibson RS, Ryan JM, Gascho JA, Watson DD, Beller GA. Prevalence of high-risk thallium-201 scintigraphic findings in left main coronary artery stenosis: Comparison with patients with multiple- and single-vessel coronary artery disease. Am J Cardiol 1984;53:462-9.
12. Gimelli A, Liga R, Duce V, Kusch A, Clemente A, Marzullo P. Accuracy of myocardial perfusion imaging in detecting multivessel coronary artery disease: A cardiac CZT study. J Nucl Cardiol 2016;24:687-95.
13. Desai D, Kozeski G, Akinboboye O. Detection of multivessel coronary artery disease: Looking beyond the extent of perfusion abnormalities. J Nucl Cardiol 2009;16:4-5.

14. Duvernoy CS, Ficaro EP, Karabajakian MZ, Rose PA, Corbett JR. Improved detection of left main coronary artery disease with attenuation-corrected SPECT. J Nucl Cardiol 2000;7:639-48.
15. Patil HR, Bateman TM, McGhie AI, Burgett EV, Courter SA, Case JA, et al. Diagnostic accuracy of high-resolution attenuation-corrected Anger-camera SPECT in the detection of coronary artery disease. J Nucl Cardiol 2014;21:127-34.
16. Corbett JR, Ficaro EP. Clinical review of attenuation-corrected cardiac SPECT. J Nucl Cardiol 1999;6:54-68.
17. Corbett JR, Kritzman JN, Ficaro EP. Attenuation correction for single photon emission computed tomography myocardial perfusion imaging. Curr Cardiol Rep 2004;6:32-40.
18. Ficaro EP, Fessler JA, Shreve PD, Kritzman JN, Rose PA, Corbett JR. Simultaneous transmission/emission myocardial perfusion tomography. Diagnostic accuracy of attenuation-corrected ^{99m}Tc-sestamibi single-photon emission computed tomography. Circulation 1996;93:463-73.
19. Maeda HNT, Yamaki N, Shirakawa S, Kikukawa K, Toyama H, et al. Attenuation correction for myocardial SPECT: Segmentation with scatter and photopeak window data for attenuation correction (SSPAC) method. J Nucl Med 2002;43:230.
20. Okuda K, Nakajima K, Motomura N, Kubota M, Yamaki N, Maeda H, et al. Attenuation correction of myocardial SPECT by scatter-photopeak window method in normal subjects. Ann Nucl Med 2009;23:501-6.
21. Yamauchi Y, Kanzaki Y, Otsuka K, Hayashi M, Okada M, Nogi S, et al. Novel attenuation correction of SPECT images using scatter photopeak window data for the detection of coronary artery disease. J Nucl Cardiol 2014;21:109-17.
22. Germano G, Kavanagh PB, Slomka PJ, Van Kriekinge SD, Pollard G, Berman DS. Quantitation in gated perfusion SPECT imaging: The Cedars-Sinai approach. J Nucl Cardiol. 2007;14:433-54.
23. Cerqueira MD, Weissman NJ, Dilsizian V, Jacobs AK, Kaul S, Laskey WK, et al. Standardized myocardial segmentation and nomenclature for tomographic imaging of the heart. A statement for healthcare professionals from the Cardiac Imaging Committee of the Council on Clinical Cardiology of the American Heart Association. Circulation 2002;105:539-42.
24. Tonino PA, Fearon WF, De Bruyne B, Oldroyd KG, Leesar MA, Ver Lee PN, et al. Angiographic versus functional severity of coronary artery stenoses in the FAME study fractional flow reserve versus angiography in multivessel evaluation. J Am Coll Cardiol 2010;55:2816-21.
25. Yonetsu T, Murai T, Kanaji Y, Lee T, Matsuda J, Usui E, et al. Significance of microvascular function in visual-functional mismatch between invasive coronary angiography and fractional flow reserve. J Am Heart Assoc 2017;6:e005916.
26. McLaughlin MG, Danias PG. Transient ischemic dilation: A powerful diagnostic and prognostic finding of stress myocardial perfusion imaging. J Nucl Cardiol 2002;9:663-7.
27. Weiss AT, Berman DS, Lew AS, Nielsen J, Potkin B, Swan HJ, et al. Transient ischemic dilation of the left ventricle on stress thallium-201 scintigraphy: A marker of severe and extensive coronary artery disease. J Am Coll Cardiol 1987;9:752-9.
28. Heller GV, Links J, Bateman TM, Ziffer JA, Ficaro E, Cohen MC, et al. American Society of nuclear cardiology and society of nuclear medicine joint position statement: Attenuation correction of myocardial perfusion SPECT scintigraphy. J Nucl Cardiol 2004;11:229-30.
29. Verberne HJ, Acampa W, Anagnostopoulos C, Ballinger J, Bengel F, De Bondt P, et al. EANM procedural guidelines for radionuclide myocardial perfusion imaging with SPECT and SPECT/CT: 2015 revision. Eur J Nucl Med Mol Imaging 2015;42:1929-40.
30. Huang JY, Huang CK, Yen RF, Wu HY, Tu YK, Cheng MF, et al. Diagnostic performance of attenuation-corrected myocardial perfusion imaging for coronary artery disease: A systematic review and meta-analysis. J Nucl Med 2016;57:1893-8.
31. Dorbala S, Di Carli MF, Delbeke D, Abbara S, DePuey EG, Dilsizian V, et al. SNMMI/ASNC/SCCT guideline for cardiac SPECT/CT and PET/CT 1.0. J Nucl Med 2013;54:1485-507.
32. Hendel RC, Berman DS, Cullom SJ, Follansbee W, Heller GV, Kiat H, et al. Multicenter clinical trial to evaluate the efficacy of correction for photon attenuation and scatter in SPECT myocardial perfusion imaging. Circulation 1999;99:2742-9.
33. Yusuf S, Zucker D, Peduzzi P, Fisher LD, Takaro T, Kennedy JW, et al. Effect of coronary artery bypass graft surgery on survival: Overview of 10-year results from randomised trials by the coronary artery bypass graft surgery trialists collaboration. Lancet 1994;344:563-70.
34. Melikian N, De Bondt P, Tonino P, De Winter O, Wyffels E, Bartunek J, et al. Fractional flow reserve and myocardial perfusion imaging in patients with angiographic multivessel coronary artery disease. JACC Cardiovasc Interv 2010;3:307-14.
35. Forster S, Rieber J, Ubleis C, Weiss M, Bartenstein P, Cumming P, et al. Tc-99 m sestamibi single photon emission computed tomography for guiding percutaneous coronary intervention in patients with multivessel disease: A comparison with quantitative coronary angiography and fractional flow reserve. Int J Cardiovasc Imaging 2010;26:203-13.
36. Ragosta M, Bishop AH, Lipson LC, Watson DD, Gimple LW, Sarembock IJ, et al. Comparison between angiography and fractional flow reserve versus single-photon emission computed tomographic myocardial perfusion imaging for determining lesion significance in patients with multivessel coronary disease. Am J Cardiol 2007;99:896-902.
37. Takx RA, Blomberg BA, El Aidi H, Habets J, de Jong PA, Nagel E, et al. Diagnostic accuracy of stress myocardial perfusion imaging compared to invasive coronary angiography with fractional flow reserve meta-analysis. Circ Cardiovasc Imaging 2015;8:e002666.